

Heavy Fermion Stabilization of Solitons in 1+1 Dimensions

E. Farhi^a, N. G. Graham^{a,b}, R. L. Jaeger^a, and H. W. Weigel^a

^aCenter for Theoretical Physics, Laboratory for Nuclear Science, and Department of Physics
Massachusetts Institute of Technology, Cambridge, Massachusetts 02139
and

^bDragon Systems, Inc., Newton, MA 02460
MIT-CTP # 2950

Abstract

We find static solitons stabilized by quantum corrections in a (1+1)-dimensional model with a scalar field chirally coupled to fermions. This model does not support classical solitons. We compute the renormalized energy functional including one-loop quantum corrections. We carry out a variational search for a configuration that minimizes the energy functional. We find a nontrivial configuration with fermion number whose energy is lower than the same number of free fermions quantized about the translationally invariant vacuum. In order to compute the quantum corrections for a given background field we use a phase-shift parameterization of the Casimir energy. We identify orders of the Born series for the phase shift with perturbative Feynman diagrams in order to renormalize the Casimir energy using perturbatively determined counterterms. Generalizing dimensional regularization, we demonstrate that this procedure yields a finite and unambiguous energy functional.

1. INTRODUCTION

Many quantum field theories contain solitons, nontrivial configurations that are local minima of the energy functional. Often, the existence of a soliton can be anticipated from topological properties of the field theory. In such cases, topologically nontrivial configurations cannot be continuously deformed into a vacuum configuration. The existence of a conserved charge suggests that a classical soliton remains stable when quantum effects are included. Still, a detailed look at the dynamics is required to see that such configurations do not collapse to a point. In general, the question of soliton stability requires a detailed study of the energy. If we have a reliable method for computing the leading quantum contributions to the energy of nontrivial field configurations, we can begin to study the stability

e-mail: farhi@mit.edu, graham@pierre.mit.edu, jaeger@mit.edu, weigel@ctp.mit.edu
Heisenberg Fellow

of topological and nontopological solitons. The techniques introduced in Ref. [4] provide such a framework in renormalizable quantum field theories.

In this paper we apply these techniques to reexamine suggestions made in previous works [5,6] that a heavy fermion can create a soliton. We consider a simple renormalizable quantum field theory in 1+1 dimensions. In this model, a two-component scalar field couples to fermions in a chirally invariant way. The fermion mass arises from a Yukawa coupling to the scalar, which has a nonzero vacuum expectation value. At the classical level the theory has no solitons. We investigate whether configurations of the scalar field that carry fermion quantum numbers can be lighter than ordinary fermion states built on top of the translationally invariant vacuum. We show that they can, and that the lightest of these configurations can be identified as a stable soliton.

It is well known that a fermion can be strongly bound in the background of a spatially varying scalar field. But the binding energy comes with the cost of the classical energy of the scalar configuration. In addition, there is the possible cost of an increase of the fermion Casimir energy, since the fermion vacuum is polarized by the background scalar field. We must include this contribution because it is of the same order in the loop-counting parameter as the binding energy of the strongly bound level.

We give a detailed description of our method for calculating the one-loop fermion contribution to the energy of a fixed scalar background. Our method is exact for an arbitrary spatially varying background. It sums all orders in the derivative expansion. Since we work in a renormalizable theory, our results are unambiguous; we use the same counterterms in the presence of the soliton that we determined from the renormalization conditions in the perturbative sector. In order to combine the infinite loop energy and the infinite counterterm contribution into a finite answer, we must regularize the theory. Phase shifts are a key ingredient in our approach. The Casimir energy is the sum over the energy shift of each mode in the fixed background. We express the sum over modes as an integral over the continuum density of states, which we relate in turn to the phase shifts. Then the ultraviolet-divergent pieces of the loop energy are linked to low orders of the Born series for the phase shifts, which can be unambiguously identified with Feynman diagrams. In this framework the quantum corrections to the energy are expressed as the sum of two finite pieces: a momentum integral involving Born-subtracted phase shifts, and perturbatively renormalized Feynman diagrams [3].

The (1+1)-dimensional model we consider has many features in common with the linear model in 3+1 dimensions: renormalizability, chirally symmetric scalar-fermion interactions, an asymmetric spectrum of the Dirac Hamiltonian, and a topological structure. Hence our findings in the (1+1)-dimensional case suggest that similar phenomena might occur in 3+1 dimensions: heavy fermions can be realized as soliton configurations carrying fermion number. This result is in agreement with decoupling theorems [6], which show that solitons supply the necessary fermion numbers to maintain anomaly cancellation after a fermion is decoupled by increasing its Yukawa coupling.

In a theory with N_F fermions, quantum corrections due to boson loops are suppressed by N_F relative to the fermion quantum corrections. Therefore we work with N_F large. However, boson loops require special attention in a (1+1)-dimensional model with (classical) spontaneous symmetry breaking. Because of infrared singularities, the symmetry is actually restored by these corrections and it would be inappropriate to construct a soliton about a

classical minimum. To circumvent this difficulty we introduce an explicit symmetry breaking term that is large enough to guarantee a unique vacuum state. Other treatments of solitons at the quantum level based on the inverse scattering method [7,9] cannot accommodate this essential ingredient.

Our paper is organized as follows: In Section 2 we introduce the scalar sector of the model and explain the necessity of explicitly breaking the chiral symmetry. Section 3 contains the discussion of the fermionic sector. In Section 4 we combine the scalar and fermion sectors to form the full expression for the energy. The corresponding numerical results are presented in Section 5. We summarize our findings in Section 6. In Appendix A we justify the phase shift method using dimensional regularization. In Appendix B we demonstrate the behavior of the strongly bound fermion level in the WKB approximation. In Appendix C we explain why the soliton background need not be reflectionless, as claimed in previous works. Some of the results presented in this paper were summarized in Ref. [10].

2. THE BOSON SECTOR

We consider a two component scalar field governed by the Lagrangian

$$L_B = \frac{1}{2} \partial_\mu \tilde{\phi} \partial^\mu \tilde{\phi} - V(\tilde{\phi}) \tag{2.1}$$

where $\tilde{\phi} = (\phi_1; \phi_2)$. The potential V contains the usual Higgs term and an explicit symmetry breaking piece proportional to ϕ_1 ,

$$V(\tilde{\phi}) = \frac{g}{8} \tilde{\phi} \tilde{\phi} + \frac{1}{2} v^2 \tilde{\phi}^2 + \frac{1}{2} \frac{v^2}{m^2} \tilde{\phi}^3 + \frac{1}{2} v^2 \phi_1 \tag{2.2}$$

If $m = 0$, the $U(1)$ transformation

$$\phi_1 + i \phi_2 \rightarrow e^{i\alpha} (\phi_1 + i \phi_2) \tag{2.3}$$

is a symmetry of L_B , but we take m big enough to avoid infrared singularities that would arise when this symmetry is spontaneously broken. For $m > 0$, $V(\tilde{\phi})$ has a unique classical minimum at $\tilde{\phi}_{cl} = (v; 0)$. The modes fluctuating about the classical vacuum have masses

$$m^2 = (m^2 + g)v^2 \quad \text{and} \quad m^2 = v^2 \tag{2.4}$$

Note that on the chiral circle, $\tilde{\phi} \tilde{\phi} = v^2$, this model reduces to the sine-Gordon model.

Although we are principally interested in the stabilizing effects of fermions, we must first consider the infrared singularities in the boson sector that could invalidate our approach. We wish to study scalar field configurations that are deformations of the classical vacuum. However, it is well known that when $m = 0$, spontaneous symmetry breaking does not occur [11]. The absence of long-range order in 1+1 dimensions can be traced to infrared singularities associated with the propagator of the massless mode. Making m big enough gives mass to the would-be Goldstone mode and stabilizes the classical vacuum.

The infrared problems can be seen in the renormalized one-loop effective potential, V_e^B ,

$$V_e^B(\tilde{\phi}) = \frac{1}{16} \left[\frac{h}{2} \ln \frac{2}{m^2} + \frac{h}{2} \ln \frac{2}{m^2} \right] m^2 \tag{2.5}$$

where λ^2 are the eigenvalues of the 2×2 matrix $\partial^2 V = \partial_i \partial_j$:

$$\lambda^2(\tilde{v}^2) = \frac{1}{2} (2\tilde{v}^2 - \tilde{v}^2 - \tilde{v}^2 + 2\tilde{v}^2) = \tilde{v}^2 : \quad (2.6)$$

We have renormalized V_e^B so that the vacuum expectation value at $\tilde{v} = \tilde{v}_{cl}$ and the particle masses m and m' remain unchanged. As $\tilde{v} \rightarrow 0$, $m^2 \rightarrow 0$, so V_e^B develops a logarithmic infrared divergence reflecting the fluctuations that restore $U(1)$ invariance. But for any nonzero \tilde{v} , V_e^B is well defined and has a unique minimum at \tilde{v}_{cl} .

When we consider the fermion one-loop contribution, we find that when \tilde{v} becomes small the character of configurations that minimize the energy changes. To see this, note that $V_e^B(\tilde{v}) = 0$ for any scalar field configuration on the chiral circle. As $\tilde{v} \rightarrow 0$, \tilde{v} is forced to the chiral circle because any other choice has infinite energy. On the other hand, for a slowly varying \tilde{v} that circles zero once as x goes from -1 to $+1$, the classical energy goes to zero if \tilde{v} stays on the chiral circle and the scale over which \tilde{v} varies gets large. This nontrivial field configuration has zero boson contribution to its energy through one loop in the limit $\tilde{v} \rightarrow 0$. (Since the configuration varies slowly, integrating eq. (2.5) over x gives a good approximation to the one-loop effective energy; because we are in 1+1 dimensions, all higher derivative terms go to zero as the scale over which \tilde{v} varies gets large.) When we consider the fermion one-loop contribution to the energy of this configuration, we find that it too contributes zero. Furthermore this configuration has fermion number one. Thus as $\tilde{v} \rightarrow 0$ the model has a zero-energy, infinitely large soliton carrying fermion number. We believe this object is destroyed by the fluctuations that restore $U(1)$ invariance. In our numerical search for solitons, we find a sharp transition as we vary \tilde{v} . At small \tilde{v} , we find that configurations with large widths are energetically favored, and the width is controlled by \tilde{v} . At large \tilde{v} we find configurations with moderate widths are favored, and the width is no longer sensitive to changes in \tilde{v} . We are interested in the latter.

3. THE FERMION SECTOR

The purpose of this section is fourfold. First, we set up the formal expression for the contribution of the fermion sector to the energy, which is expressed through the eigenvalues of the single-particle Dirac equation. Second, we set up the formalism for solving the Dirac equation in a general background $\tilde{v}(x)$. We show how to obtain the phase shifts, which characterize the continuum states. Third, we explain how the properly regulated and renormalized fermion one-loop contribution to the energy can be computed in terms of the phase shifts and the bound state energies. And fourth, we explain how the fermion number of the background \tilde{v} can be computed in terms of the phase shifts and bound states.

A. The Fermion Casimir Energy

We introduce N_F Dirac fermions coupled in a chirally invariant way to \tilde{v} . We suppress the flavor label, but keep track of factors of N_F as necessary,

$$L_F = \frac{i}{2} \bar{\psi} \not{\partial} \psi - \frac{G}{2} \bar{\psi} \psi ; \quad \psi_1 + i \psi_5 ; \quad \psi_2 : \quad (3.1)$$

The fermions acquire mass $m = Gv$ when the boson field takes the vacuum value $\tilde{\phi}_{cl}$. We have been careful about operator ordering in eq. (3.1) because of its role in determining the fermionic contribution to the vacuum energy. The ordering of anticommuting fermion fields is fixed by requiring charge conjugation invariance. We define $C_1 = \gamma_1, C_2 = \gamma_2$, and choose a Majorana basis for the Dirac matrices, $\gamma_0 = \gamma_2, \gamma_1 = i\gamma_3$, and $\gamma_5 = \gamma_4$, so that $C = \gamma_5$. With these definitions it is easy to verify that $[\psi; \psi]$ is even under C and that $[\psi; \psi_5]$ and $[\psi; \psi_4]$ are odd under C .

Given the ordering in eq. (3.1), the second quantized Hamiltonian becomes $H[\tilde{\phi}] = \frac{1}{2} \int dx [\psi^\dagger; H(\tilde{\phi}) \psi]$, where $H(\tilde{\phi})$ is the single-particle Dirac Hamiltonian in the presence of $\tilde{\phi}(x)$. Denoting the (positive and negative) energy eigenvalues of H by ϵ_n , and the corresponding eigenfunctions by ψ_n , we make the usual Fock decomposition, $\psi(x; 0) = \sum_{\epsilon_n > 0} b_n \psi_n(x) + \sum_{\epsilon_n < 0} d_n^\dagger \psi_n(x)$, so that

$$H[\tilde{\phi}] = \frac{1}{2} \sum_{\epsilon_n > 0} \epsilon_n (b_n^\dagger b_n - b_n b_n^\dagger) + \frac{1}{2} \sum_{\epsilon_n < 0} \epsilon_n (d_n d_n^\dagger - d_n^\dagger d_n) : \quad (3.2)$$

We are interested in the expectation value of $H[\tilde{\phi}]$ in states of definite occupation number. Consider the vacuum state $|j\rangle$, characterized by $b_n |j\rangle = d_n |j\rangle = 0$. Then

$$E^F[\tilde{\phi}] = \langle j | H[\tilde{\phi}] | j \rangle = \frac{1}{2} \sum_n \epsilon_n |j_n| : \quad (3.3)$$

Of course this sum is divergent. Its regularization and renormalization are discussed below.

It is easy to confirm that $|j\rangle$ is the lowest energy state. We see that the vacuum energy in a charge conjugation invariant theory is given by the (regularized) sum over the absolute values of all single-particle states. This result can be verified [12] using functional integral techniques, where it follows from the evaluation of the path integral for large Euclidean times. The fermion number of $|j\rangle$ depends on $\tilde{\phi}$, and for many configurations of interest it is not zero.

For completeness, we write out the one-loop fermion vacuum contribution to the effective potential,

$$V_e^F(\tilde{\phi}) = \frac{G^2 n}{4} \int \tilde{\phi}^2 \ln \tilde{\phi}^2 = v^2 \int \tilde{\phi}^2 : \quad (3.4)$$

Of course, our principal motivation in this work is to go beyond the effective potential approximation for the fermion one-loop contribution to the energy. Nevertheless, eq. (3.4) will be useful to verify our numerical results for the fermion one-loop vacuum contribution in the case of a slowly varying boson fields. Also, like the boson effective potential, V_e^F vanishes on the chiral circle, as we anticipated in the discussion of the $\tilde{\phi} \rightarrow 0$ limit in the previous section.

B. Solutions to the Dirac Equation in a Chiral Background

The Dirac Hamiltonian is

$$H[\tilde{\phi}] = i \gamma_1 \frac{d}{dx} + G_2 \gamma_1(x) + G_3 \gamma_2(x) : \quad (3.5)$$

Although the underlying theory is charge conjugation invariant, the Dirac Hamiltonian in the presence of a fixed $\tilde{\psi}(x)$ is not. Thus it is necessary to consider both positive and negative energy eigenvalues ϵ of the time-independent Dirac equation

$$H\psi = \epsilon\psi \quad (3.6)$$

The associated second-order equations for the Dirac spinor, $\begin{pmatrix} f \\ g \end{pmatrix}$, are

$$\begin{aligned} \epsilon^2 f + G_1^0 f + G_2^0 (\epsilon + G_2)^{-1} (\epsilon^2 f + G_1^0 f) &= (\epsilon^2 - G_1^2 - G_2^2) f \\ \epsilon^2 g + G_1^0 g - G_2^0 (\epsilon - G_2)^{-1} (\epsilon^2 g - G_1^0 g) &= (\epsilon^2 - G_1^2 - G_2^2) g \end{aligned} \quad (3.7)$$

In one dimension, there are two channels for each energy. The S-matrix is 2-dimensional and, in general, not diagonal. We simplify this situation using parity invariance. By demanding that ψ_1 and ψ_2 are respectively even and odd under coordinate reflection, i.e., $\psi_1(x) = \psi_1(-x)$ and $\psi_2(x) = -\psi_2(-x)$, we ensure that the Dirac Hamiltonian, eq. (3.5), is invariant under parity,

$$[P; H] = 0; \quad \text{where } P = \sigma_x \quad (3.8)$$

and σ_x is the coordinate reflection operator that transforms x to $-x$. Thus we can choose a basis of parity eigenstates,

$$P\psi(x) = \pm\psi(x) \quad (3.9)$$

Using parity we can replace the scattering problem on the line $x \in [-1; 1]$ by two scattering problems on the half-line $x \in [0; 1]$ corresponding to even and odd parity. Eq. (3.9) gives boundary conditions at $x = 0$ on the parity eigenstates:

$$\psi_+(0) = \frac{1}{i} \psi_+'(0) \quad \text{and} \quad \psi_-(0) = \frac{1}{i} \psi_-'(0) \quad (3.10)$$

The solution to the Dirac equation on the half-line with either boundary condition is unique up to an overall normalization. For $x \gg 1$, this unique solution can be written as a superposition of incoming ($\propto e^{ikx}$) and outgoing ($\propto e^{-ikx}$) waves. The coefficient of the outgoing wave relative to the incoming wave defines the phase shift.

To implement this program, we introduce eigenstates of the free Dirac Hamiltonian with energy ϵ ,

$$\begin{aligned} \psi_{+k}^0(x) &= \frac{1}{\sqrt{k^2 + m^2}} e^{ikx} \\ \psi_{-k}^0(x) &= \frac{1}{\sqrt{k^2 + m^2}} e^{-ikx} \end{aligned} \quad (3.11)$$

where $k = \sqrt{\epsilon^2 - m^2}$. Next, we construct the eigenstates of the full interacting Dirac Hamiltonian with energy ϵ that are asymptotic to $\psi_{\pm k}^0$ as $x \gg 1$,

$$\psi_{+k}(x) = \frac{1}{\sqrt{k^2 + m^2}} (f^0(x) + G_1(x)f(x)) \quad (3.12)$$

and

$$f_k(x) = \frac{i}{k + G_2(x)} (f^0(x) + G_1(x)f(x)) \quad (3.13)$$

where $f(x)$ is the solution to the real second-order equation, eq. (3.7), for the upper component, subject to the boundary condition that $f(x) \sim e^{ikx}$ as $x \rightarrow 1$. It is easy to verify that in the same limit $f_k(x) \sim f_k^0(x)$ since the boson fields approach their vacuum values.

Since the even and odd parity channels decouple, the S -matrix is diagonal. Its diagonal elements $S_{\pm} = e^{2i\delta_{\pm}(k)}$ can be defined through the even and odd parity eigenstates of H ,

$$\begin{aligned} \psi_+(x) &= f_k(x) + \frac{m}{k} \frac{ik}{k} S_+(k) f_{+k}(x) \\ \psi_-(x) &= f_k(x) - \frac{m}{k} \frac{ik}{k} S_-(k) f_{+k}(x) : \end{aligned} \quad (3.14)$$

If we set the interaction to zero ($G_1 = v; G_2 = 0$), then $\psi_{\pm}(k)$ reduces to the even (odd) parity solution to the free Dirac equation with $S_{\pm} = 1$, which explains the extra factor of $\frac{m}{k}$ in eq. (3.14).

To determine S_{\pm} we use the fact that the eigenstates of eq. (3.14) obey eq. (3.10). For the positive parity channel this yields

$$S_+(k) = \frac{(m + ik) [(k - G_1(0))f(0) - f^0(0)]}{k [(k - G_1(0))f(0) - f^0(0)]} \quad (3.15)$$

and similarly for the negative parity channel

$$S_-(k) = \frac{(m + ik) [(k + G_1(0))f(0) + f^0(0)]}{k [(k + G_1(0))f(0) + f^0(0)]} : \quad (3.16)$$

To compute the phase shifts efficiently and avoid 2π ambiguities, it is convenient to factor the free solution out of $f(x)$ by writing $f(x) = e^{ikx} e^{i\phi(x;k)}$. Then the phase shifts are given by

$$\delta_{\pm}(k) = \text{Re} \phi(0;k) \pm \frac{1}{2} \arg \left[1 + \frac{i \phi^0(0;k) + G_1(0) - v}{k + m + ik} \right] \quad (3.17)$$

where the complex function $\phi(x;k)$ solves the differential equation

$$\begin{aligned} i \phi''(x;k) + 2k \phi'(x;k) + \phi^2(x;k) - m^2 + G_1^2(x) + G_2^2(x) - G_1^0(x) \\ + \frac{G_2^0(x)}{k + G_2(x)} G_1(x) + i(k + \phi^0(x;k)) = 0 \end{aligned} \quad (3.18)$$

subject to the boundary conditions $\phi(1;k) = \phi^0(1;k) = 0$. It is this equation that we solve numerically for a given background $\tilde{\phi}(x)$ to determine the phase shifts.

C. Fermion One-Loop Contribution to the Effective Energy

Having explained how to obtain the phase shifts for positive and negative energies and parities, we next show how to compute the fermion quantum corrections to the soliton energy following the method of [13].

The difference $E^F[\tilde{\psi}]$ between the fermion one-loop contribution to the effective energy in the background of $\tilde{\psi}$ and in the trivial background $\tilde{\psi}_{cl}$ is given formally by the shift in the zero-point energies of the fermion modes, $\frac{1}{2} \sum_j (\epsilon_j - \epsilon_{j0})$, where ϵ_{j0} are the eigenenergies in the free case. We rewrite this formal expression as a sum over bound states and an integral over k weighted by $\rho(k) - \rho_0(k)$, the difference between the density of states in the free and the interacting cases, giving

$$E^F[\tilde{\psi}] = \frac{1}{2} \sum_j \epsilon_j - \frac{1}{2} \sum_{j_0} \epsilon_{j_0} + \int_0^{\infty} dk \, \rho(k) \sqrt{k^2 + m^2} (\rho(k) - \rho_0(k)) \frac{m}{2} + E_{ct} \quad (3.19)$$

where $\epsilon_{j_0} \in [-m; m]$ denote the discrete bound states. The extra $m=2$ takes into account the contribution from the threshold states at $\epsilon = \pm m$ in the free case [13]. E_{ct} is the contribution from the counterterm Lagrangian, which is evaluated at tree level. A counterterm proportional to $\tilde{\psi} \tilde{\psi}$ is implicitly present in eq. (2.1), which must be renormalized due to the coupling to the fermions.

Both the counterterms and the integral over the continuum are formally infinite. Since our model is renormalizable, the sum is finite. In order to avoid ambiguities associated with the separate divergent terms in eq. (3.19) we have extended the method of dimensional regularization to this representation of the effective energy: Eq. (3.19) and the subsequent development should be understood as defined in n dimensions, where all integrals are convergent and all counterterms are finite. All the manipulations that we perform in the rest of this section are unambiguous in n dimensions. The final result is then analytically continued back to 1+1 dimensions, where it remains finite. Since this extension of dimensional regularization is new and may have wider application, we present it in a self-contained way in Appendix A.

The difference between the free and interacting density of states is given in terms of the scattering phase shifts by

$$\rho(k) - \rho_0(k) = \frac{1}{2\pi} \frac{d}{dk} \delta_F(k) \quad (3.20)$$

where

$$\delta_F(k) = \delta_+^+(\epsilon_k) + \delta_+^-(\epsilon_k) + \delta_-(\epsilon_k) + \delta_-(\epsilon_k) \quad (3.21)$$

and $\epsilon_k = \sqrt{k^2 + m^2}$. $\delta_F(k)$ sums the contributions from positive and negative energies and both parities. As in [13], we use Levinson's theorem

$$\begin{aligned} \delta_+^+(m) + \delta_+^-(m) &= \left(n^+ - \frac{1}{2}\right) \\ \delta_-(m) + \delta_-(m) &= \left(n^- - \frac{1}{2}\right) \end{aligned} \quad (3.22)$$

to relate the phase shifts at $k = 0$ in each channel to the number of bound states in that channel. The factors of $\frac{1}{2}$ are peculiar to one dimension and reflect the existence of bound

states at threshold in the absence of interactions. For a complete discussion, see Refs. [2] and [13]. Levinson's theorem enables us to rewrite

$$E_F[\tilde{\Gamma}] = \frac{1}{2} \sum_j (j! j!) + \frac{1}{2} \int_0^{Z-1} dk \sqrt{k^2 + m^2} \frac{d}{dk} F(k) \frac{m}{2} + E_{ct} \quad (3.23)$$

as

$$E_F[\tilde{\Gamma}] = \frac{1}{2} \sum_j (j! j! - m) + \int_0^{Z-1} \frac{dk}{2} \sqrt{k^2 + m^2} - m \frac{d}{dk} F(k) + E_{ct} \quad (3.24)$$

In terms of the shifted field $h = \frac{1}{2} v$, the counterterm contribution to eq. (3.24) is

$$E_{ct} = C \int_0^Z (h^2 + 2hv + \frac{v^2}{2}) dx \quad (3.25)$$

consistent with the chiral symmetry of the fermion interaction. We fix the coefficient C by the renormalization condition that the counterterm exactly cancels the tadpole graph (the term linear in h), and we perform no further finite renormalizations. This chooses the counterterm contribution to be equal to the tadpole graph plus those parts of the graphs with two external lines that are related to the tadpole graph by eq. (3.25). This contribution is entirely local, i.e., independent of the external momenta. In order to reexpress this contribution in terms of phase shifts, we use the Born series. We expand the phase shifts in powers of the external fields h and v . The contribution from the tadpole graph corresponds to the contribution from the first Born approximation to the phase shift. Expanding eq. (3.17) and eq. (3.18) to lowest order in h and v we find that the first Born approximation is given by

$$F^{(1)}(k) = F_+^{(1)}(k) + F_+^{(1)}(k) + F^{(1)}(k) + F^{(1)}(k) = \frac{4G^2 v}{k} \int_0^{Z-1} h(x) dx \quad (3.26)$$

Once we have fixed the term linear in h , the entire counterterm contribution to the phase shift is fixed by eq. (3.25) to be

$$\hat{F}_F(k) = \frac{2G^2 v}{k} \int_0^{Z-1} dx v^2 \tilde{\Gamma}(x)^2 \quad (3.27)$$

Subtracting $\hat{F}_F(k)$ from $F_F(k)$ in eq. (3.24) then implements the full contribution of the counterterm, giving

$$E_F[\tilde{\Gamma}] = \frac{1}{2} \sum_j (j! j! - m) + \int_0^{Z-1} \frac{dk}{2} \sqrt{k^2 + m^2} - m \frac{d}{dk} F(k) - \hat{F}_F(k) \quad (3.28)$$

By expanding eq. (3.17) and eq. (3.18) for large k we see that $\hat{F}_F(k)$ gives the leading $1/k$ behavior of $F_F(k)$ for k large, and thus the resulting integral over the continuum is finite. We note that on the chiral circle $v^2 = v^2$, the counterterm contribution (3.27) to the energy vanishes, implying that the one-loop quantum contribution to the energy is finite. This is a consequence of the chiral invariance of the boson-fermion interaction, which forces the

counterterms involving the "would-be" Goldstone boson to contain at least two derivative operators. On dimensional grounds these counterterms must be finite in 1+1 dimensions. In the present context, it implies that $\Gamma_F(k)$ decreases more rapidly than $1/k$ as $k \rightarrow 1$ for scalar configurations on the chiral circle, and our numerical computation indicates that in this case $\Gamma_F(k)$ goes like $1/k^3$ for k large.

For numerical computations, it is convenient to integrate eq. (3.28) by parts, yielding

$$E^F[\tilde{\phi}] = \frac{1}{2} \sum_j (j! j^j - m) + \int_0^{\infty} \frac{dk}{2} \frac{k}{k^2 + m^2} \Gamma_F(k) \hat{\Gamma}_F(k) : \quad (3.29)$$

This is the finite expression for the fermion one-loop contribution to the effective energy which we evaluate numerically. The analysis of the first part of this section gives us the phase shifts, and we find the bound states by ordinary shooting methods, with Levinson's theorem telling us how many to look for.

D. The Fermion Number of a Configuration

We are interested in fermionic solitons and therefore must keep track of the fermion number. If, as we adiabatically turn on the background configuration starting from the trivial vacuum, a fermion level crosses zero from above, the vacuum will have this state filled, giving the configuration a positive fermion number. (If the crossing is in the other direction, there is a negative fermion number.) The fermion energy levels are N_F -fold degenerate, so the configuration carries each of the N_F fermion numbers. We know from general considerations that if $\tilde{\phi}(x)$ circles $\tilde{\phi} = (0;0)$ as $\tilde{\phi}$ goes from $(v;0)$ at $x = -1$ to $(v;0)$ at $x = 1$, then the vacuum state will carry nonzero fermion number provided that w , the scale over which $\tilde{\phi}$ varies, is much larger than the fermion Compton wavelength $1/m$ [6,14].

In Ref. [4] we show how to compute this fermion number directly using Levinson's theorem, which relates the phase shifts at $\epsilon = m$ to the total number of bound states. We use that the difference between the phase shift at the positive energy threshold, $\epsilon = m$, and the actual number of positive (negative) energy bound states $n_>$ ($n_<$) counts the fermion number Q of the vacuum :

$$\begin{aligned} Q[\tilde{\phi}] &= N_F \left[\frac{1}{2} + (m) + (m) + \frac{1}{2} n_> \right] \\ &= N_F \left[\frac{1}{2} + (m) + (m) + \frac{1}{2} n_< \right] : \end{aligned} \quad (3.30)$$

As noted above, the extra $\frac{1}{2}$ is peculiar to one dimension, and is essential to get correct (integer) values for Q . States at the respective thresholds count as $\frac{1}{2}$ in $n_>$ or $n_<$. The configurations that we consider circle $\tilde{\phi} = (0;0)$ at most once, so Q is either 0 or N_F .

We are interested in states with fermion number N_F . If $Q = N_F$, then the state we want is the vacuum. If $Q = 0$, then we build the lowest energy state with fermion number N_F by filling the lowest positive energy level ϵ_1 of eq. (3.5) with N_F fermions. Thus the total fermionic contribution to the energy is

$$E^F = E^F + \epsilon_1(N_F - Q) : \quad (3.31)$$

We note that E^F varies smoothly with μ_1 even as μ_1 crosses zero. The vacuum and valence contributions each have discontinuities in slope when $\mu_1 = 0$, but the contribution from this level is $\frac{1}{2}j_1$ from the vacuum energy in eq. (3.29) plus $\mu_1(j_1)$ as a filled valence level. The sum is $\frac{1}{2}j_1$ for all μ_1 , which is smooth.

The spectrum also contains states with total charge between zero and N_F . These states are constructed by an appropriate filling of the tightly bound level if $\mu_1 > 0$ or the emptying of that level if $\mu_1 < 0$. We do not consider such states because their binding will be smaller than that of states with charge N_F . We note, however, that if the effects we find in the large N_F limit persist for moderate values of N_F , then in that case a stable soliton with fermion number 1 would represent an elementary fermion.

It will also be helpful to consider the fermion charge density. The vacuum contribution is given by summing over the eigenstates obtained from eq. (3.14),

$$\langle j^y(x) \rangle = N_F \int_{-\infty}^{\infty} \text{sgn}(\mu) \frac{1}{2} \left[\psi_+^y(x) \psi_+^\dagger(x) + \psi_-^y(x) \psi_-^\dagger(x) \right] d\mu \quad (3.32)$$

where the integral over μ includes both continuum and bound states. We have restored the suppressed μ label on the wavefunctions and normalized them by

$$\int_{-\infty}^{\infty} \psi^\dagger(x) \psi(x) dx = \delta(\mu - \mu^0) \quad (3.33)$$

where the right hand side is interpreted as a Dirac delta function for continuum states and a Kronecker delta for bound states. The norm of the scattering states is related to the phase shifts by

$$\int_{-\infty}^{\infty} \psi^\dagger(x) \psi(x) dx = \frac{1}{d\mu} \frac{d\delta(\mu)}{d\mu} \quad (\text{for } j_1 > m) \quad (3.34)$$

as derived in [2]. The spatial integral over the bound state contribution to (3.32) yields the difference between the numbers of positive and negative energy bound states, $n_+ - n_-$. Thus by integrating eq. (3.32) over x and using Levinson's theorem and the fact that the total number of states is unchanged, we obtain eq. (3.30).

If $Q = 0$ we have to explicitly add the contribution of the level $\psi_1(x)$ with the lowest positive eigenvalue. Thus the total charge density is given by

$$\langle j^y(x) \rangle = (N_F - Q) \psi_1^y(x) \psi_1^\dagger(x) + \langle j^y(x) \rangle_{\text{vac}} \quad (3.35)$$

4. THE TOTAL ENERGY

Now that the theory has been prescribed by $L_B + L_F$, it is useful to introduce dimensionless variables to simplify our analysis. We measure all energies in units of the perturbative fermion mass, $m = Gv$, and all distances in terms of $\xi = m^{-1}x$. We are interested in calculating the energy of a fixed background configuration $\tilde{\phi}(x)$, which we describe in terms of a small set of dimensionless variational parameters f_{ij} . Next we rescale $\tilde{\phi}$ by v (both of which are dimensionless in one dimension) so that $\tilde{\phi} \sim (1;0)$ as $j \rightarrow 1$, and we define dimensionless couplings

$$\tilde{g} = \frac{g}{G^2} \quad \text{and} \quad \tilde{h} = \frac{h}{G^2} \quad (4.1)$$

With all these rescalings the boson classical energy can be written as

$$\begin{aligned} \frac{E_{\text{cl}}[\tilde{\phi}]}{m} &= v^2 \int_{-1}^1 dx \left[\frac{1}{2} \tilde{\phi}'^2 + \frac{1}{8} \tilde{\phi}^4 \right] \left(1 + \frac{2\tilde{\phi}^2}{\tilde{g}} \right) \sim (1) \\ &= v^2 E_{\text{cl}}(\tilde{\phi}; \tilde{g}; f_{\text{ig}}) \end{aligned} \quad (4.2)$$

where prime denotes a derivative with respect to x .

The fermion one-loop contribution to the energy is given by a regulated sum over the absolute values of the eigenfrequencies, f_{ng} , of $H[\tilde{\phi}]$. Once we measure distances in units of \tilde{g} and choose dimensionless variational parameters f_{ig} , the perturbative fermion mass factors out of the Dirac Hamiltonian, so its eigenvalues f_{ng} scale with m . In all, the fermion one-loop vacuum energy can be written as

$$E^{\text{F}}[\tilde{\phi}] = N_{\text{F}} m E^{\text{F}}(f_{\text{ig}}) : \quad (4.3)$$

Thus we compute

$$\frac{E_{\text{tot}}[\tilde{\phi}]}{N_{\text{F}} m} = \frac{v^2}{N_{\text{F}}} E_{\text{cl}}(\tilde{\phi}; \tilde{g}; f_{\text{ig}}) + E^{\text{F}}(f_{\text{ig}}) : \quad (4.4)$$

This computation is exact in the limit $N_{\text{F}} \rightarrow 1$ and $v^2 \rightarrow 1$ with the ratio $v^2 = N_{\text{F}}$ held fixed, since the contributions we have neglected all arise from loops with internal bosons, which are suppressed by v^2 relative to the classical energy and by N_{F} relative to the one-loop fermion energy.

To compare the energy of our background configuration to the energy of the state with the same charge built on top of the translationally invariant vacuum, we study the effective energy per fermion minus N_{F} times the perturbative fermion mass gv , which we denote as $B[\tilde{\phi}]$. In terms of rescaled variables,

$$B \frac{v^2}{N_{\text{F}}}; \tilde{\phi}; \tilde{g}; f_{\text{ig}} = \frac{v^2}{N_{\text{F}}} E_{\text{cl}}(\tilde{\phi}; \tilde{g}; f_{\text{ig}}) + E^{\text{F}}(f_{\text{ig}}) - 1 : \quad (4.5)$$

A field configuration with $B < 0$ is energetically favored over the state with the same charge N_{F} built on top of the translationally invariant vacuum.

5. NUMERICAL EXPLORATIONS

In this section we present the results of our numerical studies. We will show that the model has a stable fermionic soliton for a wide range of the model parameters \tilde{g} , \tilde{v} , and $v^2 = N_{\text{F}}$. For fixed model parameters, we search over the variational parameters looking for a bound solitonic fermion. The classical contribution to the soliton energy, E_{cl} in eq. (4.5), is positive and is scaled by $v^2 = N_{\text{F}}$. The fermion one-loop contribution, $E^{\text{F}} - 1$, is generically negative. Thus, the existence of a stable fermionic soliton can be discussed in terms of a maximum value of $v^2 = N_{\text{F}}$ for a given choice of \tilde{g} and \tilde{v} .

A. Variational Ansatz

We choose an ansatz $\tilde{\psi}_I(\mathbf{r})$ characterized by the parameters R and w ,

$$\tilde{\psi}_I(\mathbf{r}; R; w) = \frac{1}{R} \left(1 + R \cos \frac{\mathbf{r} \cdot \hat{\mathbf{z}}}{w}; R \sin \frac{\mathbf{r} \cdot \hat{\mathbf{z}}}{w} \right) \quad (5.1)$$

with

$$\frac{\mathbf{r} \cdot \hat{\mathbf{z}}}{w} = \arctan \left(\frac{R \sin \theta}{1 + R \cos \theta} \right) \quad (5.2)$$

For fixed R and w , $\tilde{\psi}_I$ describes a circle centered at $(1, 0)$ with radius R as θ varies. w gives the characteristic size of the configuration. Varying R allows us to interpolate between the trivial vacuum, $\tilde{\psi} = (1; 0)$, and a configuration that circles the origin once while staying on the chiral circle, $|\tilde{\psi}| = 1$. Configurations with $R > 1$ go beyond the chiral circle. When the symmetry breaking parameter \tilde{m} is large, $\tilde{\psi} = (1; 0)$ is energetically disfavored, leading to a preference for R to go to zero to avoid that point.

We have also considered other ansätze, but we found that they yielded variational minima that had comparable or higher energy. Thus we will restrict our attention to this choice.

B. Stability Studies

To search for the soliton, we must compute the classical energy $E_{cl}(\tilde{\psi}; \tilde{\psi}; R; w)$ and the fermionic contribution $E^F(R; w)$. Our scaling has simplified the numerical ansatz by putting all the dependence on the model parameters \tilde{m} , \tilde{g} , and $v^2 = N_F$ into the classical energy, which is easy to compute. The fermionic contribution, which is harder to compute, depends only on the variational parameters R and w .

The classical energy is computed from eq. (4.2). A typical energy surface for ansatz $\tilde{\psi}_I$ is shown in Fig. 1 as a function of R and w for a generic choice of model parameters, \tilde{m} and \tilde{g} .

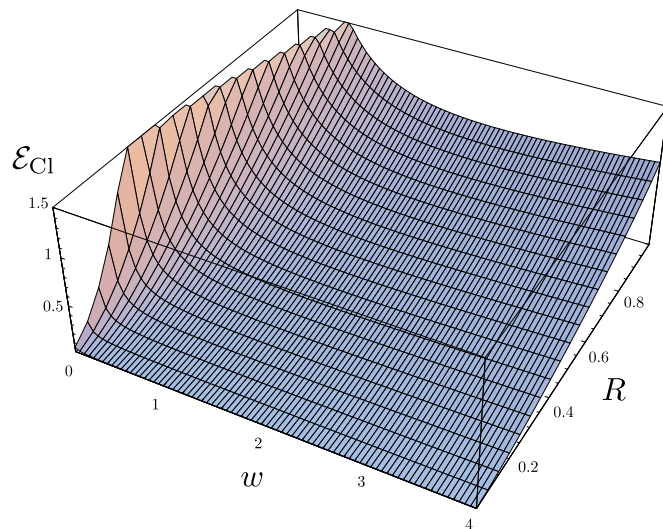


FIG. 1. The classical energy, E_{cl} , as a function of the variational parameters R and w in eq. (4.2). The parameters of the bosonic Lagrangian are $\tilde{m} = 1.0$ and $\tilde{g} = 0.5$.

Simple scaling arguments allow us to understand the principal features of Fig. 1. For fixed w , $E_{\text{cl}}(\tilde{\psi}; \tilde{\psi}; R; w)$ vanishes as $R \rightarrow 0$ because the ansatz approaches the classical vacuum for all $\tilde{\psi}$. For fixed $R \notin 0$, $E_{\text{cl}}(\tilde{\psi}; \tilde{\psi}; R; w)$ diverges like $1/w$ for small w due to the $\tilde{\psi}^0 \tilde{\psi}^2$ terms in eq. (4.2). For large w , $E_{\text{cl}}(\tilde{\psi}; \tilde{\psi}; R; w)$ grows linearly with w for fixed $R \notin 1$ because $V(\tilde{\psi})$ is nonzero in a region of size w .

Next we turn to the fermion contribution to the energy. There are two distinct contributions discussed in the previous section: first, the energy of any "valence" levels, and second the vacuum energy. An important property of our ansatz is its propensity to bind a fermion. This can be seen in Fig. 2, where we plot the lowest fermion eigenenergy ω_1 as a

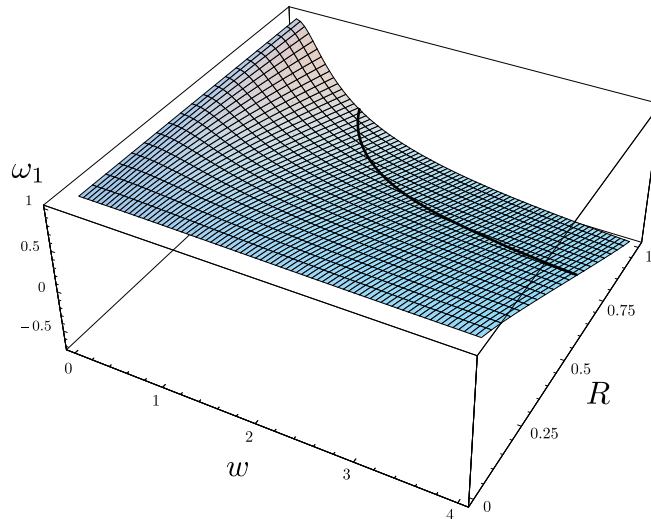


FIG. 2. The lowest quark eigenenergy, ω_1 , for ansatz $\tilde{\psi}_I$, as a function of R and w . Note that for large R and w , ω_1 is negative. A solid curve marks the contour $\omega_1 = 0$.

function of the variational parameters R and w for the ansatz $\tilde{\psi}_I$. Since we are using scaled variables the fermion continuum begins at $\omega = 1$. Notice that for R near 1, which puts $\tilde{\psi}_I$ close to the chiral circle, the lowest fermion eigenenergy decreases quickly with increasing w . Even a modest value of w leads to a negative eigenenergy.

The strongly bound fermion state drives the formation of a fermionic soliton. The situation is reminiscent of the appearance of a fermion zero mode in the presence a soliton in a theory of a real scalar field [15]. It is expected from considerations of level crossings in the presence of an adiabatically changing field: If we fix $R > \frac{1}{2}$ so that the orbit in the $(\psi_1; \psi_2)$ plane circles the origin, then as w increases from 0 to 1 one fermion level must cross from the positive to the negative continuum [6,14]. Our numerical studies indicate that ω_1 is never negative unless the orbit of $\tilde{\psi}$ circles the origin.

In Appendix B, we explore the generality of level crossings for field configurations on the chiral circle. We show that the WKB approximation yields a single strongly bound level in the positive parity channel, which crosses from the positive to negative continuum as the width is increased. Note that merely examining the spectrum in the limit of large width gives no evidence of the level crossing. It is essential to follow the levels as a function of width or use the Levinson's theorem method, eq. (3.30).

Next we calculate the contribution from the fermionic vacuum { the Casimir energy { given by eq. (3.29). Note that this sum over the eigenenergies of the Dirac Hamiltonian is

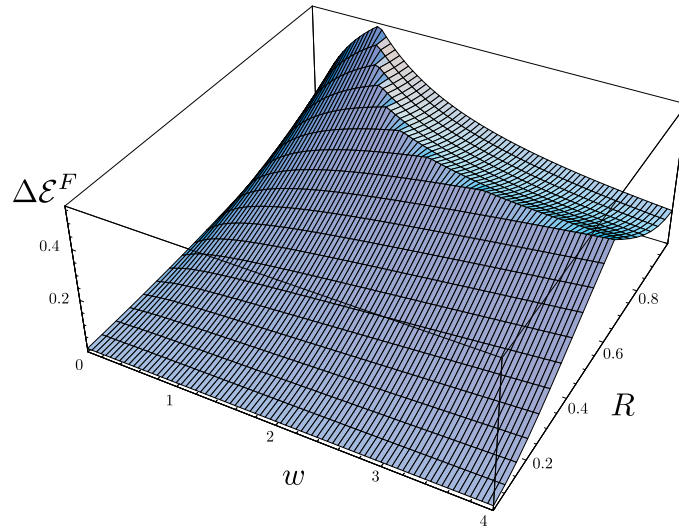


FIG. 3. The vacuum contribution to the one-loop fermion energy as a function of R and w . The sharp edge in this contribution occurs when the lowest fermion eigenvalue crosses zero. See Fig. 2.

of the same order in $v^2 = N_F$ as the energy of the lowest eigenmode and must be included in a consistent calculation of the one-loop fermion contribution to the effective energy. This piece of the energy is also a function only of the ansatz parameters R and w . It is shown in Fig. 3. It displays a discontinuity in slope at the point where the lowest eigenvalue passes through zero. Fig. 4 shows that the sum of the Casimir energy and the contribution from

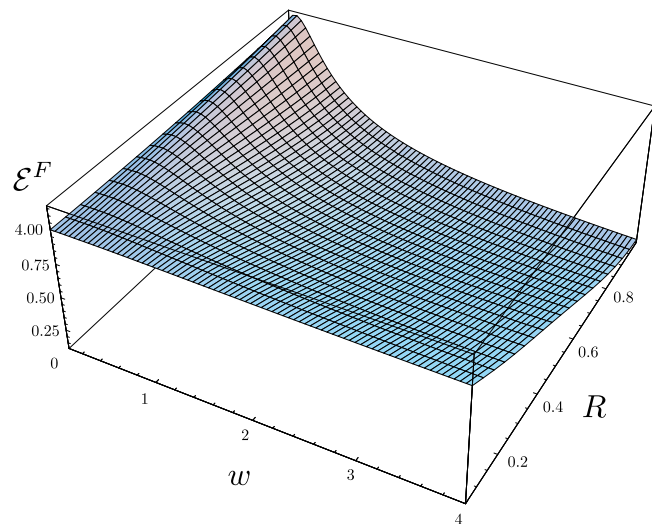


FIG. 4. The fermion one-loop contribution, $E^F(R; w)$, to the energy of a state of fermion number N_F for the ansatz I.

ϕ_1 is smooth, in agreement with the discussion in the previous section.

Finally, we combine the classical energy and the one-loop fermion energy to form $B(v^2 = N_F; \tilde{m}; \tilde{g}; f; g)$ and search for a stable fermionic soliton. As an example of our results, Fig. 5 shows B as a function of R and w for $\tilde{m} = 1$, $\tilde{g} = 0.50$, and $v^2 = N_F = 0.375$.

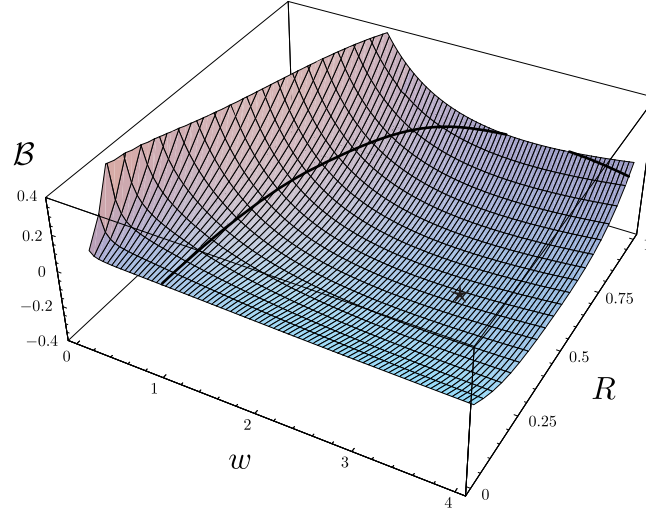


FIG. 5. B as a function of the ansatz parameters for $\tilde{m} = 0.5$, $\tilde{v} = 1.0$, and $v = \frac{p}{N_F} = 0.375$. A solid curve marks the contour $B = 0$, and a star indicates the minimum at $w = 2.808$ and $R = 0.586$.

$B < 0$ is the signal of a stable fermionic soliton. The domain of negative B is large and the variational approximation to the fermionic soliton lies at the minimum: $R = 0.586$, $w = 2.808$. In this case the lowest fermion eigenenergy, $\epsilon_1 = 0.0985$, is slightly positive so this level must be filled. The variational approximation to the binding energy is 0.253. In Fig. 6 we show $\rho_1(x)$, $\rho_2(x)$, and $j(x)$. We see that the charge density is well localized around the center of the soliton.

We are now in a position to study the stability of the fermionic soliton as a function of the model parameters \tilde{m} , \tilde{v} , and $v^2 = N_F$. For each choice of parameters we minimize B over the ansatz parameters, R and w . The output is $B(\tilde{m}; \tilde{v}; v^2 = N_F)$ and the parameters $R(\tilde{m}; \tilde{v}; v^2 = N_F)$ and $w(\tilde{m}; \tilde{v}; v^2 = N_F)$ that minimize B . In Fig. 7 we plot B versus $v = \frac{p}{N_F}$ for various choices of \tilde{m} and \tilde{v} and see that binding occurs over a wide range of model parameters. Binding is a quantum phenomenon: it is maximal when $v = \frac{p}{N_F}$, which multiplies the classical contribution, vanishes, and decreases with increasing $v = \frac{p}{N_F}$.

The dependence on the explicit symmetry breaking parameter \tilde{m} is particularly important because of the infrared problem we expect to arise as $\tilde{m} \rightarrow 0$. Fig. 7 confirms our expectation that $B \rightarrow 1$ (strong binding) as $\tilde{m} \rightarrow 0$. However this is a suspect limit. A look at the width of the soliton displays the problem. This is shown in Fig. 8 where w and R are plotted versus \tilde{m} for various choices of \tilde{v} and a typical value of $v = \frac{p}{N_F}$. Two qualitatively different regimes are separated at $\tilde{m}_0 \approx 0.3$. Above \tilde{m}_0 the size of the soliton is almost independent of \tilde{m} . Below \tilde{m}_0 the width of the soliton diverges like $1/\tilde{m}$ and the ansatz moves towards the chiral circle, $R = 1$. However, this is where we expect the model to be invalidated by infrared divergences generated by the would-be Goldstone mode. Therefore we only trust our results in the domain $\tilde{m} > \tilde{m}_0$. We have made plots analogous to Fig. 6 for various choices of \tilde{m} and $v = \frac{p}{N_F}$. We find that \tilde{m}_0 depends weakly on \tilde{v} but strongly on $v = \frac{p}{N_F}$. In Fig. 9 we plot $\tilde{m}_0(v = \frac{p}{N_F})$ defined as the point where the break occurs in figures analogous to Fig. 6. In the absence of a complete analysis of the infrared problem as $\tilde{m} \rightarrow 0$, we only trust our results when $\tilde{m} > \tilde{m}_0(v = \frac{p}{N_F})$.

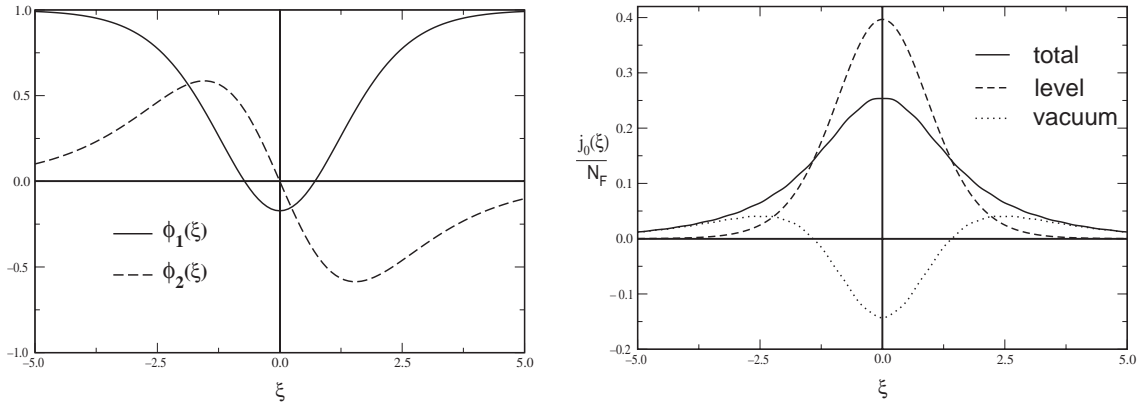


FIG. 6. ϕ_1 , ϕ_2 , and the fermion number density j_0 at the variational minimum for $\tilde{\alpha} = 0.5$, $\tilde{\alpha} = 1.0$, and $v = \frac{p}{N_F} = 0.375$, which is at $R = 0.586$, $w = 2.808$. The left panel shows $\phi_1(\xi)$ and $\phi_2(\xi)$ at this point, and the right panel shows $j_0(\xi)$, which gets contributions from both the fermion vacuum and the filled valence level.

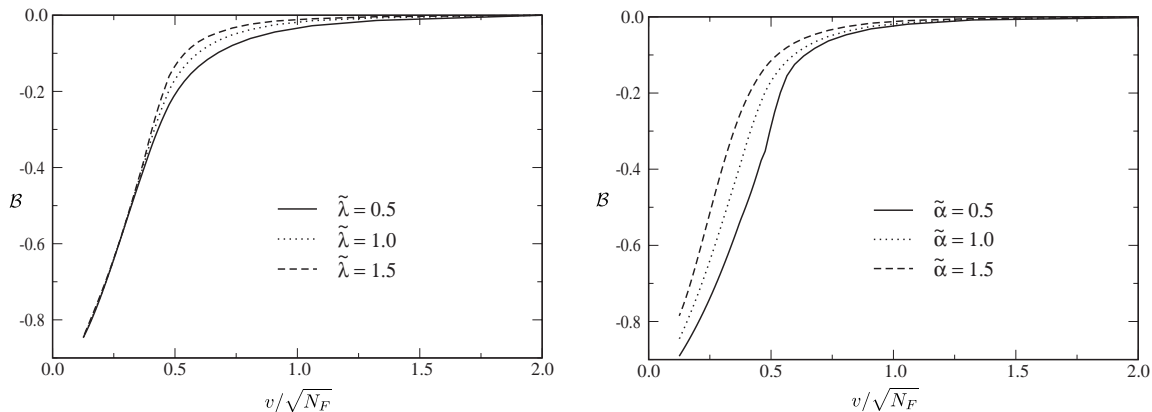


FIG. 7. B as a function of $v = \frac{p}{N_F}$ for various values $\tilde{\alpha}$ with $\tilde{\alpha} = 0.25$ (left panel) and for various values $\tilde{\alpha}$ with $\tilde{\alpha} = 1.0$ (right panel).

For fixed $\tilde{\alpha}$, when $v = \frac{p}{N_F}$ is too small we run into the infrared instabilities we described above. When $v = \frac{p}{N_F}$ is very large the soliton binding becomes small. The interesting domain is between these two extremes where a stable soliton can be reliably described. To indicate this domain we have added a contour corresponding to 5% binding in Fig. 9. In between we have found a strongly bound fermionic soliton.

6. DISCUSSION AND CONCLUSIONS

We have shown that quantum effects can stabilize a soliton in a theory with no soliton at the classical level. In order to convincingly demonstrate this phenomenon, it is necessary to consider a renormalizable model. We study a (1+1)-dimensional model with a chirally invariant Yukawa interaction between fermions and scalars. The scalar self-interaction is given by a Higgs potential with an explicit symmetry breaking term. (Without the explicit symmetry breaking, the fluctuations of the Goldstone modes would restore the spontaneously

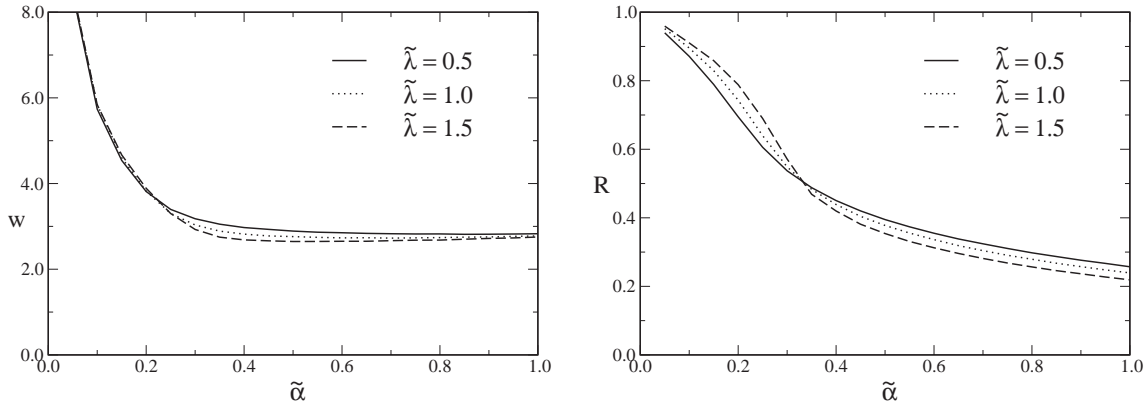


FIG. 8. The width (left panel) and the radius (right panel) of the configurations that minimize the total energy as a function of the explicit symmetry breaking $\tilde{\alpha}$. Several values of the Higgs coupling constant $\tilde{\lambda}$ are considered and $v = \frac{p}{N_F} = 0.375$.

broken symmetry.) We define the renormalized energy functional using counterterms determined in the perturbative sector of the theory. Our phase shift formalism allows us to unambiguously include the exact fermion one-loop quantum corrections in a manner that is computationally tractable. The omission of the scalar loop contribution is justified by assuming a large number of fermion flavors.

Holding the total fermion number fixed, we performed a variational calculation to search for configurations with lower energy than the same number of free fermions. Once we have found a bound configuration we are assured that a stable soliton exists since its energy can only be smaller than the variational minimum. As expected, when the typical extension of the background field is large compared to the Compton wavelength of the noninteracting fermion, the fermion number is carried intrinsically by the background field, instead of through explicitly filled levels.

We have found a wide range of model parameters for which we believe that the soliton is not destroyed by the infrared singularities of the "would-be" Goldstone mode, and where the binding of the variational minimum is sizable. In this case, the cost in the classical energy is more than compensated by the gain from the fermion loop. For a fixed set of the dimensionless model parameters, the gain in energy is proportional to the dimensionful Yukawa coupling constant G , and the phenomenon of soliton formation becomes more pronounced as the perturbative mass of the fermion increases. Thus, in 1+1 dimensions, heavy fermions can indeed stabilize solitons.

Acknowledgments

We would like to thank S. Bashinsky, J. Goldstone, and D. Son for helpful conversations, suggestions, and references. We thank J. Feinberg and A. Zee for helpful correspondence related to their work. This work is supported in part by funds provided by the U.S. Department of Energy (D.O.E.) under cooperative research agreement # DF-FC 02-94ER 40818 and the Deutsche Forschungsgemeinschaft (DFG) under contract We 1254/3-1.

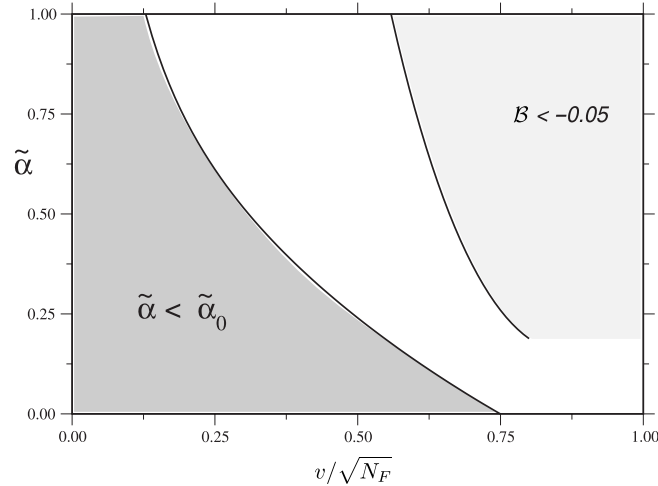


FIG. 9. The regions of soliton stability in the plane of $v/\sqrt{N_F}$ and $\tilde{\alpha}$. In the shaded area on the left, a growing width indicates potential infrared instabilities. In the shaded area on the right, the soliton is bound by less than 5 percent. In between, we have a stable, tightly bound soliton.

APPENDIX A : DIMENSIONAL REGULARIZATION OF THE CASIMIR ENERGY

In the body of the paper we introduced and manipulated formally divergent expressions such as eq. (3.19) without prescribing a regularization scheme to render them finite. For Feynman diagrams, regularization and renormalization are so familiar that such a casual approach would not warrant further comment. In this Appendix we show how to extend the method of dimensional regularization to Casimir sums, thereby rendering our earlier manipulations well defined. This analysis resolves ambiguities in the definition of the effective energy that have been noted in recent works [16].

We begin by defining the Casimir energy in n (space) dimensions in terms of a sum over bound states and an integral over a continuum density of states. These are properties of a radial Schrodinger-like equation, which remain well defined when n is noninteger. We choose n such that the expressions are finite. We then isolate and compute the term $E^{(1)}$ that diverges when n is continued to $n = 1$, the case of interest. For $0 < n < 1$ we show explicitly that $E^{(1)}$ is identical to the contribution of the lowest order Feynman diagram in the loop expansion of the effective energy. This is our fundamental result. Still keeping $0 < n < 1$ we subtract $E^{(1)}$ from the Casimir sum and add back in the Feynman diagram. The subtracted Casimir sum is finite for $n = 1$ while the now (conventionally) dimensionally regulated Feynman diagram is renormalized by the counterterm contribution, E_{ct} . This calculation demonstrates that we have precisely implemented the standard dimensional regularization and renormalization process of perturbative field theory.

For simplicity we consider the self-interactions of a single real boson in one dimension; the generalization to fermions is straightforward. We take the bosonic Lagrangian

$$L = \frac{1}{2} \partial_\mu \phi \partial^\mu \phi - U(\phi) + C U^{(0)}(\phi) \quad (\text{A } 1)$$

where prime denotes differentiation with respect to ϕ . We have indicated the counterterm $C U^{(0)}(\phi)$ explicitly including its cutoff-dependent coefficient C , and we are considering an

arbitrary potential $U(\phi)$. This counterterm renormalizes the boson's mass, and is the only counterterm needed to render the theory finite in one spatial dimension. We take a background $\phi_0(x)$ that is either a solution to the classical equations of motion or held in place by an external source, so that it is a stationary point of the classical action. We wish to compute the one-loop contribution to the energy arising from the bosonic fluctuations about $\phi_0(x)$. To simplify the analysis, we assume it is either an odd or an even function of x , and we take $U(\phi)$ to be an even function of ϕ that gives a perturbative mass m to ϕ . The potential for small oscillations around $\phi_0(x)$ is then given by

$$V(x) = U''(\phi_0(x)) : \quad (\text{A.2})$$

Our restrictions on $U(\phi)$ and $\phi_0(x)$ ensure that $V(x)$ is even in x . As usual, the relationship between the scattering phase shifts and the density of states is

$$\rho(k) = \frac{1}{2\pi i} \text{Tr} \ln S = \frac{1}{2\pi} \frac{d}{dk} \delta(k) : \quad (\text{A.3})$$

For a single real field ϕ , we only need to consider positive energies. We use parity to decompose the S -matrix into symmetric and antisymmetric channels, giving

$$B(k) = B^+(k) + B^-(k) : \quad (\text{A.4})$$

As in Section III we define the Casimir energy as the sum over bound states f_j plus an integral over the continuum weighted by $\omega = \sqrt{k^2 + m^2}$,

$$E[\tilde{\phi}] = \frac{1}{2} \sum_j (\omega_j - m) + \frac{1}{2} \int_0^\infty dk (\omega - m) \rho(k) + E_{\text{ct}} \quad (\text{A.5})$$

where in analogy to eq. (3.19) we have used Levinson's theorem to regulate potential infrared divergences (as $k \rightarrow 0$).

We now generalize eqs. (A.3) and (A.5) to n dimensions. The scattering problem generalizes to a central potential in n dimensions. The S -matrix is diagonal in the basis of the irreducible tensor representations of $SO(n)$. These are the traceless symmetric tensors of rank λ , where $\lambda = 0; 1; 2; \dots$. The formula for the density of states, eq. (A.3), becomes a sum over λ ,

$$\rho_n(k) = \frac{1}{2\pi} \frac{d}{dk} B_n(k) = \frac{1}{2\pi} \frac{d}{dk} \sum_{\lambda=0}^{\infty} N_{n,\lambda} \delta_{\lambda}(k) \quad (\text{A.6})$$

where $\delta_{\lambda}(k)$ is the phase shift in the λ^{th} partial wave and $N_{n,\lambda}$ is the degeneracy of the $SO(n)$ representation labelled by λ . For integer n and λ , $N_{n,\lambda}$ is given by the dimension of the space of symmetric tensors with λ indices that each run from 1 to n , with all traces (contractions) removed. Working out the combinatorics gives

$$N_{n,\lambda} = \frac{(n + \lambda - 1)!}{\lambda!(n - 1)!} \frac{(n + \lambda - 3)!}{(\lambda - 2)!(n - 1)!} : \quad (\text{A.7})$$

To prepare the way to continue to noninteger n we write N_n in terms of Γ -functions instead of factorials,

$$N_n = \frac{(n + \frac{1}{2})}{(n - 1) (\frac{1}{2} + 1)} (n + 2)^{-2} : \tag{A.8}$$

For $n = 3$, N_n reduces to $2^{-1} + 1$ as expected.

The phase shifts are obtained by solving the radial Schrodinger equation generalized to n dimensions,

$$\omega \frac{n - 1}{r} + \frac{1}{r^2} + \frac{V(r)}{r^2} + 2m V(r) = k^2 \tag{A.9}$$

which is related to Bessel's equation for $V = 0$. At the origin, the regular solution $h_{n,\ell}$ is proportional to r^ℓ independent of n .

Incoming and outgoing waves are generalizations of spherical Hankel functions,

$$h_{n,\ell}^{(1;2)}(kr) = \frac{1}{(kr)^{\frac{n}{2} - 1}} J_{\frac{n}{2} + \ell - 1}(kr) \pm i Y_{\frac{n}{2} + \ell - 1}(kr) \tag{A.10}$$

and the phase shifts are defined in the usual way by writing the solution $h_{n,\ell}$ regular at the origin as

$$h_{n,\ell} = h_{n,\ell}^{(2)}(kr) + e^{2i\delta_{n,\ell}(k)} h_{n,\ell}^{(1)}(kr) \tag{A.11}$$

for large r , where the potential vanishes. The leading behavior of $\delta_{n,\ell}(k)$ at large k is given by the first Born approximation,

$$\delta_{n,\ell}^{(1)}(k) = -\frac{1}{2} \int_0^\infty J_{\frac{n}{2} + \ell - 1}^2(kr) V(r) r dr : \tag{A.12}$$

Thus the expression for the Casimir energy in n dimensions is

$$E_n[\tilde{\Gamma}] = \frac{1}{2} \sum_j \sum_{\ell=0}^{\infty} N_n(\ell, j, n) + \sum_0^{\infty} \frac{dk}{2} \sum_{\ell=0}^{\infty} N_n \frac{d}{dk} \delta_{n,\ell}(k) + E_{ct,n} \tag{A.13}$$

where N_n is given by eq. (A.8), the $\psi_{j,m,\ell}$ are the normalizable solutions to eq. (A.9) in each partial wave ℓ , and $\delta_{n,\ell}(k)$ is determined from eqs. (A.9) and eq. (A.11). $E_{ct,n}$ is the counterterm contribution, to be fixed by a renormalization condition below. The rest of eq. (A.13) is well defined for noninteger n , where the integration over k and the sum over ℓ converge. Holding the divergences in abeyance we can verify that eq. (A.13) reduces to the naive result, eq. (A.5), as $n \rightarrow 1$: N_1 vanishes for all ℓ except $\ell = 0$ and $\ell = 1$, where it is 1; for $\ell = 0$, $\psi_{j,0,0}(k)$ and $\psi_{j,1,0}$ are obtained from the solutions to eq. (A.8) that have vanishing first derivative at $r = 0$, while for $\ell = 1$, $\psi_{j,1,1}(k)$ and $\psi_{j,1,1}$ are obtained from the solutions to eq. (A.8) that vanish at $r = 0$. Thus $\ell = 0$ and $\ell = 1$ correspond to the even and odd parity channels respectively.

Our approach consists of subtracting the first Born approximation to the phase shift and replacing its contribution by the tadpole graph, which we then calculate in ordinary Feynman perturbation theory. Thus we must demonstrate explicitly that these two quantities are equal

by computing both as analytic functions of n , away from integer n , where both diverge. Once the leading Born approximation has been subtracted, the integral over the phase shift is finite and we can take the limit $n \rightarrow 1$ with no further subtleties.

The tadpole graph requires the external momentum to be equal to zero. Thus we should expect that both the leading Born approximation and the tadpole graph will depend only on the spatial average of the potential,

$$\langle hV \rangle = \int_0^Z V(x) dx = \frac{2}{\frac{n}{2}} \int_0^Z V(r) r^{\frac{n}{2}-1} dr : \quad (\text{A.14})$$

From eq. (A.13), the contribution to the energy from the first Born approximation is

$$E^{(1)}[\tilde{\gamma}] = \int_0^X \int_0^Z \frac{dk}{2} (i - m) \frac{d_{n,i}^{(1)}(k)}{dk} : \quad (\text{A.15})$$

We obtained $(i - m)$ rather than i in the integrand of eq. (A.15) because of our use of Levinson's theorem to put the Casimir energy in the form of eq. (A.5). This manipulation was required to ensure the absence of infrared singularities in one spatial dimension, but we will see that it is also necessary for us to write a sensible expression in arbitrary dimensions.¹

Using the Bessel function identity

$$\int_0^X \frac{(2q+2\ell)(2q+\ell)}{(\ell+1)} J_{q+\ell}(z)^2 = \frac{(2q+1)}{(q+1)^2} \frac{z^{2q}}{2} \quad (\text{A.16})$$

and setting $q = \frac{n}{2} - 1$, we explicitly sum over ℓ in eq. (A.15) and obtain

$$E^{(1)}[\tilde{\gamma}] = \frac{\langle hV \rangle}{(4)^{\frac{n}{2}}} \int_0^Z \int_0^X (i - m) k^{n-3} dk : \quad (\text{A.17})$$

The k integral can be calculated in the vicinity of $n = \frac{1}{2}$ and then analytically continued, yielding

$$\int_0^X (i - m) k^{n-3} dk = \frac{m^{n-1}}{4} = \frac{1}{2} \frac{n}{2} : \quad (\text{A.18})$$

Hence we find

$$E^{(1)}[\tilde{\gamma}] = \frac{\langle hV \rangle}{(4)^{\frac{n+1}{2}}} \frac{1}{2} m^{n-1} \quad (\text{A.19})$$

which is exactly what we obtain using standard dimensional regularization for the tadpole diagram in $n+1$ space-time dimensions.

¹If the boson were massless, we would have found an infrared divergence in eq. (A.5) as $n \rightarrow 1$ from the $1/k$ divergence of the Born approximation at $k = 0$. This divergence reflects the well-known infrared divergences of massless theories in 1+1 dimensions [1].

We choose renormalization conditions such that the tadpole graph is exactly cancelled by the counterterm contribution. Thus we can implement the contribution of $E_{ct,m}$ by subtracting $\epsilon^{(1)}(k)$ from $\epsilon_n(k)$ in eq. (A.13), yielding a finite result

$$E_n[\tilde{\epsilon}] = \frac{1}{2} \sum_j \int_{-\infty}^{\infty} N_n(\epsilon_j; m) + \int_0^{\infty} \frac{dk}{2} \int_{-\infty}^{\infty} N_n \frac{d}{dk} \epsilon_{n;l}(k) - \epsilon_{n;l}^{(1)}(k) : \tag{A.20}$$

This result can then be smoothly continued to $n = 1$, giving

$$E[\tilde{\epsilon}] = \frac{1}{2} \sum_j \int_{-\infty}^{\infty} N_1(\epsilon_j; m) + \int_0^{\infty} \frac{dk}{2} \int_{-\infty}^{\infty} \frac{d}{dk} \epsilon^B(k) - \epsilon^{(1)}(k) \tag{A.21}$$

where

$$\epsilon^{(1)}(k) = \frac{1}{k} \int_0^{\infty} V(r) dr : \tag{A.22}$$

By continuing to fractional dimensions, we have regulated the theory, rendering it finite. We made certain that we held the physical renormalization conditions fixed while removing the regulator. This process defines the theory in terms of physical parameters that can be measured within the perturbative sector. Based only on these inputs, we can then calculate the energy of nontrivial field configurations.

APPENDIX B: STUDIES OF THE TIGHTLY BOUND FERMION LEVEL

Our soliton's stability was driven largely by the strong binding of a single fermion level in a chiral background. In this appendix we explore this phenomenon further by studying the case of a scalar field constrained to the chiral circle, $\tilde{\epsilon} = (\cos(\theta); \sin(\theta))$, with the chiral angle (θ) varying monotonically between 0 and 2π as θ goes from -1 to $+1$. We assume $\theta(\theta) = \theta(\theta)$, so $\theta(0) = 0$ and $\theta'(0) > 0$. Using the WKB approximation, we argue that the vacuum will acquire unit fermion number when $\theta(\theta)$ varies slowly compared with m .

It is convenient to adopt a basis for the Dirac matrices different from the body of the paper: $\gamma^0 = \gamma_1, \gamma_1 = i\gamma_2$ and hence $\gamma_5 = \gamma_3$. Denoting the upper and lower components of the spinor by a and b , respectively, the first order Dirac equations read

$$\begin{aligned} a &= e^{-i\theta} (i b + i b^0) \\ b &= e^{i\theta} (i a - i a^0) \end{aligned} \tag{B.1}$$

where as before, the energy E is measured in units of the fermion mass, $m = Gv$ and a prime denotes a derivative with respect to $x = m x$. In this basis, the second order equations become

$$a'' = E^2 a + \theta' (i a^0 - i a) \tag{B.2}$$

$$b'' = E^2 b - \theta' (i b^0 + i b) : \tag{B.3}$$

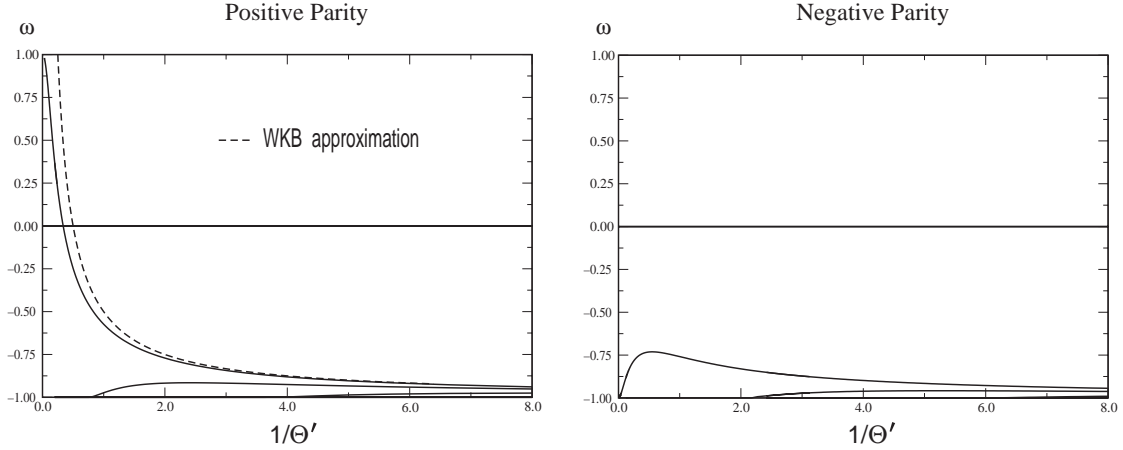


FIG. 10. The bound state energies of the simple models as functions of the inverse of the constant slope θ_0 . In the positive parity channel the WKB solution (B.6) is also shown.

A bound state is a solution to eq. (B.1) which falls exponentially as $x \rightarrow \infty$ and has definite parity: $a(0) = \pm b(0)$.

First, we suppose θ is slowly varying and use the WKB approximation. We parameterize $a(x) = e^{if^0(x)}$ and neglect f^0 compared with f^2 . Substituting into eq. (B.2) and solving for f^0 we obtain

$$f^0 = \frac{0}{2} + i \frac{q}{1} \frac{1}{\sqrt{1^2 + \theta_0^2}} \frac{1}{4} \theta^2 \quad (B.4)$$

where we have chosen the root that gives a wavefunction that falls exponentially at large x . $b(x)$ is given by the second of eqs. (B.1). The eigenvalue condition for positive (negative) parity at $x = 0$ reduces to

$$1 - f^0(0) = 1 : \quad (B.5)$$

This equation has only one solution when $\theta_0(0) > 0$,

$$1 = 1 + \theta_0(0) = 2 \quad (B.6)$$

which has positive parity. $1 = \theta_0(0)$ measures the width of the scalar field configuration. For large width, the WKB solution lies just above the negative energy continuum. As the width decreases, the WKB bound state energy increases, crosses zero when $\theta_0(0) = 2$ and enters the positive energy continuum when $\theta_0(0) = 4$.

The condition that $f^0 < f^2$ limits the validity of the WKB approximation to $\theta_0 > 1$. For example, when $\theta = 0$ the condition reduces to

$$\frac{\theta^2(x)}{4} > 1 : \quad (B.7)$$

This condition can be satisfied for all x by making θ_0 small enough. Note $\theta_0(0) = 0$ by symmetry thereby avoiding the apparent singularity at $x = 0$ where $\theta = 0$ requires $\theta_0(0) = 2$.

We have augmented the WKB analysis by solving a simple toy model where much of the calculation can be done analytically. In this model we let $\phi = \phi_0 = \text{constant}$ for $x = < -L < x = L$ and zero elsewhere. The positive and negative parity eigenstates are determined by a simple transcendental equation which can be solved numerically. The results are shown along with the WKB estimate, eq. (B.6), in Fig. 10. As expected, the toy model has a positive parity bound state that descends rapidly from the positive energy threshold, through zero energy, toward the negative energy continuum. It is well approximated by the WKB estimate. The model has other positive and negative energy bound states, which are missed by the WKB approximation, but which remain in the vicinity of either the positive or negative energy continuum for all values of L .

APPENDIX C: REFLECTION COEFFICIENTS

Ref. [8] claimed that the reflection coefficient for fermions scattering off a soliton background should vanish. Since we calculate the phase shifts $\delta(k)$, we can easily compute the reflection coefficient

$$r(k) = \frac{1}{2} [S_+(k) - S_-(k)] \tag{C.1}$$

in terms of the S-matrix elements $S_{\pm}(k) = \exp(2i\delta_{\pm}(k))$. We are thus equipped to reexamine this statement for our variational approximation to the soliton. In Fig. 11 we display the complex reflection coefficients as functions of the momentum of the scattering fermion for positive and negative energies. Although these coefficients approach zero very quickly as k increases, they do not vanish identically. In particular we find that these coefficients acquire more structure as we get closer to the (unstable) symmetric formulation ($\mu = 0$). The added structure is mainly caused by the increasing number of bound states in the wider potential. Because of Levinson's theorem these bound states cause the reflection coefficient to circle around the origin in the complex plane. Though it is still possible that the true soliton gives a reflectionless potential, we see no indication of this behavior.

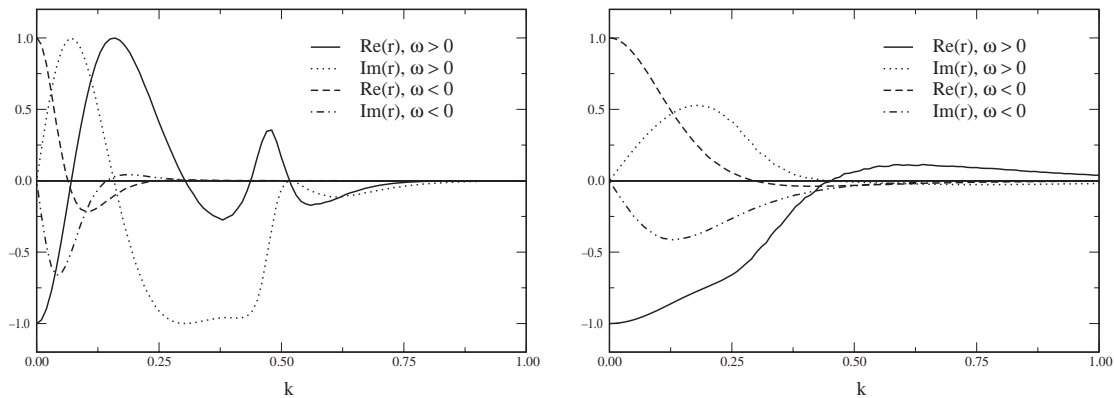


FIG. 11. The reflection coefficients of the variational approximation to the soliton as functions of the momentum $k = \frac{p}{\sqrt{1-\mu^2}}$. We consider two values of μ : 0.1 (left panel) and 0.6 (right panel). In both cases we have used $\mu = 1.0$ and $v = \frac{p}{N_F} = 0.375$, as in Fig. 6.

The statement in Ref. [8] is based on the requirement that the fermion current

$$j^1(x) = (N_F - Q) \psi^\dagger(x) \gamma^0 \gamma^1 \psi(x) + h \sum_j \psi_j^\dagger(x) \gamma^0 \gamma^1 \psi_j(x) \quad (C.2)$$

must vanish for all x in the soliton background. However, decomposing $\psi(x)$ in terms of creation and annihilation operators that multiply the solutions to the Dirac equation given in eq. (3.14), we find that $j^1(x)$ vanishes mode by mode as a simple consequence of $\beta_{+j} = \beta_{-j} = 1$ which is enforced by unitarity. Thus the requirement $j^1(x) = 0$ is trivially fulfilled and places no restriction on the soliton configuration.

Though two of the most famous examples of topological solitons, the kink and the sine-Gordon soliton, both correspond to reflectionless potentials, we have no reason to assume that such a restriction applies in general. Indeed, the Jacobi model studied in Ref. [17] gives a family of solitons labelled by the elliptic parameter ν . These solitons correspond to potentials that are not reflectionless except in the limit $\nu \rightarrow 0$ and $\nu \rightarrow 1$ (where the model reduces to the sine-Gordon case).

For certain interactions, the inverse scattering method applies and the equations of motion (expressed in terms of scattering data) indeed yields reflectionless potentials [18]. However, the attempts to extend this method to chiral models in Ref. [7,9] are problematic: First, they cannot include the symmetry breaking terms needed to avoid the restoration of chiral symmetry by boson loops. Second, because these solitons approach different configurations as $x \rightarrow -1$ and $x \rightarrow +1$ (which are degenerate vacua in the absence of symmetry breaking), the methods developed in Ref. [4,14] show that the polarized Dirac sea carries fractional charge for each fermion flavor even though no level has crossed zero. When this contribution is properly included, the total fermion number of the configuration constructed in Ref. [7] adds to zero.

REFERENCES

- [1] E. Farhi, N. G. Rajaram, P. Haagensen and R. L. Jaffe, Phys. Lett. B 427 (1998) 334.
- [2] N. G. Rajaram and R. L. Jaffe, Nucl. Phys. B 544 (1999) 432.
- [3] N. G. Rajaram and R. L. Jaffe, Nucl. Phys. B 549 (1999) 516.
- [4] E. Farhi, N. G. Rajaram, R. L. Jaffe and H. W. Eichel, "Fractional and Integer Charges from Levinson's Theorem", in preparation.
- [5] R. Mackenzie, F. Wilczek, and A. Zee, Phys. Rev. Lett. 53 (1984) 2203. G. Ripka and S. Kahana, Phys. Lett. 155B (1985) 327, Phys. Rev. D 36 (1987) 1233; R. J. Perry, Nucl. Phys. A 467 (1987) 717; B. Mousallam, Phys. Rev. D 40 (1989) 3430; G. Anderson, L. Hall, and S. G. Hsu, Phys. Lett. 249B (1990) 505; F. Wilczek, IAS preprint, IASSNS-HEP-90/20. S. Dimopoulos, B. Lynn, S. Selipsky, and N. Tetradis, Phys. Lett. 253B (1991) 237; J. Bagger and S. Naculich, Phys. Rev. Lett. 67 (1991) 2252, Phys. Rev. D 45 (1992) 1395. S. G. Naculich, Phys. Rev. D 46 (1992) 5487.
- [6] E. D. Hoker and E. Farhi, Nucl. Phys. B 248 (1984) 59, E. D. Hoker and E. Farhi, Nucl. Phys. B 248 (1984) 77.
- [7] S. Shei, Phys. Rev. D 14 (1976) 535.
- [8] J. Feinberg and A. Zee, Int. J. Mod. Phys. A 12 (1997) 1133; J. Feinberg and A. Zee, Phys. Rev. D 56 (1997) 5050.
- [9] D. K. Campbell and Yao-Tang Liao, Phys. Rev. D 14 (1976) 2093.
- [10] E. Farhi, N. G. Rajaram, R. L. Jaffe and H. W. Eichel, Phys. Lett. B 475 (2000) 335.
- [11] S. Coleman, Commun. Math. Phys. 31 (1973) 259.
- [12] R. Alkofer, H. Reinhardt, and H. W. Eichel, Phys. Rept. 265 (1996) 139.
- [13] G. Barton, J. Phys. A: Math. Gen. 18 (1985) 479;
- [14] J. Goldstone and F. Wilczek, Phys. Rev. Lett. 47 (1981) 986.
- [15] R. Jackiw and C. Rebbi, Phys. Rev. D 13 (1976) 3398.
- [16] A. Rebhan and P. van Nieuwenhuizen, Nucl. Phys. B 508 (1997) 449. H. Nastase, M. Stephanov, P. van Nieuwenhuizen and A. Rebhan, Nucl. Phys. B 542 (1999) 471.
- [17] G. V. Dunne, Phys. Lett. B 467 (1999) 238.
- [18] R. F. Dashen, R. Hasslacher, and A. Neveu, Phys. Rev. D 12 (1975) 2443.